Asymmetric Wetting Hysteresis on Chemical Defects

Craig Priest, Rossen Sedev, and John Ralston

Ian Wark Research Institute, ARC Special Research Centre for Particle and Material Interfaces, University of South Australia, Mawson Lakes, South Australia 5095, Australia

(Received 1 March 2007; published 13 July 2007)

Using the Wilhelmy plate technique, the role of chemical defects in hysteretic wetting behavior was investigated. The wetting and dewetting work differ significantly, depending on the defect energy (i.e., high or low energy with respect to the matrix). For one, or an array of high-energy defects, advancing measurements departed from equilibrium theory, while the receding data were in close agreement. Conversely for low-energy defects, only the receding measurements showed significant departure from theory. We propose that distinct wetting mechanisms for high- and low-energy defects explain the phenomenon of asymmetric hysteresis, where the advancing or receding contact angle deviates more strongly from the equilibrium angle.

DOI: 10.1103/PhysRevLett.99.026103 PACS numbers: 68.08.Bc

The wettability of inhomogeneous surfaces has attracted attention as a result of its fundamental role in many applications, including water repellency, coating or printing technologies, and mineral recovery. With rapid progress in micro and nanofabrication of specialty interfaces, e.g., biomimetics [1] and microfluidics [2], the influence of roughness and chemical heterogeneity on surface wettability has attracted greater interest from a growing interdisciplinary community. While the motivation for wetting research is continuously evolving, contact angle hysteresis has remained a central wetting phenomenon without predictive theory.

The wettability of an ''ideal'' surface can be expressed as a balance of the liquid-vapor γ, solid-liquid γ_{SL}, and solid-vapor γ_{SV} interfacial tensions, according to the well-known Young equation [3], provided the solid surface is rigid, flat, homogeneous, and inert to both fluid phases. Direct use of Young's equation is often restricted due to surface heterogeneity. Invariably, chemical heterogeneity and/or roughness must be taken into account. The focus of this Letter is the influence of chemical heterogeneity alone.

Cassie [4] accounted for chemical heterogeneity using a weighted average of the work of adhesion of each surface component. Thus, the wettability of a two-component solid can be written in terms of the contact angle:

$$\cos\theta = \phi_1 \cos\theta_1 + (1 - \phi_1)\cos\theta_2, \qquad (1)$$

where θ is the equilibrium contact angle on the heterogeneous surface, ϕ_1 is the surface area fraction of component 1, θ_1 and θ_2 are the Young contact angles for components 1 and 2, respectively. While Cassie's theory is widely accepted and often employed [5–10], efforts to apply the expression to experiments have frequently shown significant deviations [6,7,9,10]. Wetting hysteresis is, at least in part, due to chemical heterogeneity on the solid surface, for which there is no account in Cassie's equation.

To account for wetting hysteresis, Pease [11] treated the contact line as a two-dimensional ''line of tension,'' affected only by surface components in its immediate vicinity. Irregular or entirely random surface structure will complicate application of Pease's model and, possibly for that reason, few authors have adopted the approach. It is qualitatively accepted, though, that an advancing liquid will preferentially sample low-energy components, while a receding liquid will sample high-energy components, such that $\theta_a > \theta > \theta_r$.

Later, Johnson and Dettre showed that heterogeneity can introduce free energy barriers [12]. Consequently, the observed contact angle may differ markedly from Young's angle. Heterogeneity, however, does not cause wetting hysteresis in every case. Infinitely long stripes that are oriented normal to the contact line do not induce free energy barriers [12,13]. Neumann and Good proposed a general mechanism for hysteresis [13], based on rectangular defects, which is revisited here.

Consider a high-energy defect in a low-energy matrix plunging into a liquid, Fig. 1. The advancing contact line is unaffected by the defect until it arrives at the lower defect boundary ($y = 0$), when a segment of the contact line rapidly wicks up the defect to position $y = h$. The deformed contact line only returns to its original shape at the upper boundary of the defect ($y = d$) before advancing into the low-energy matrix. The receding liquid undergoes the reverse process although, owing to the liquid's higher affinity for the defect, the liquid remains pinned beyond the lower defect boundary and detachment occurs at $y < 0$. As a result, the magnitude of the dewetting energy for a high-energy defect will exceed the wetting energy. The opposite is true for a low-energy defect in a high-energy matrix.

The complexity of heterogeneous surfaces has led to a group of single defect studies [14–16]. Joanny and de Gennes [14] incorporated the elastic energy of the contact line into the mechanism of Neumann and Good [13]. In addition, the authors gave an ideal force-distance plot for a contact line passing over a high-energy defect, which takes the form of Fig. 1(b). The hysteresis energy (shaded area) can be easily quantified via integration.

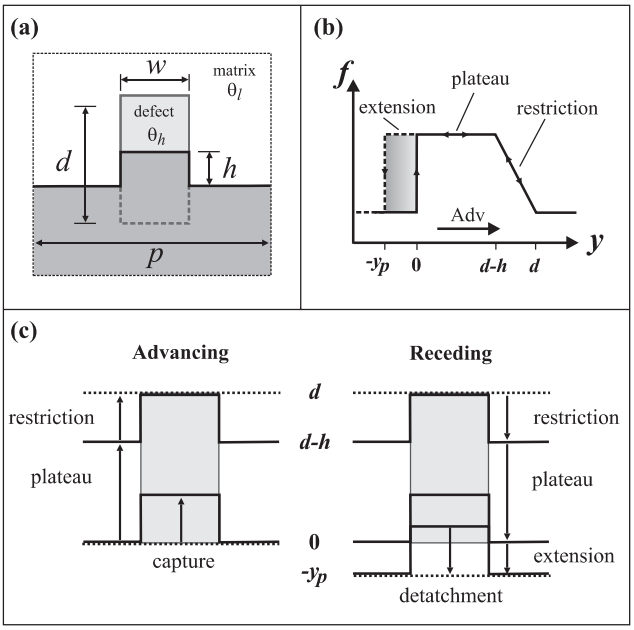

FIG. 1. (a) Schematic of liquid (dark gray) wetting a rectangular high-energy defect in a low-energy matrix. The width w and height d of the defect, capillary rise h, and perimeter of the sample p are indicated. (b) Capillary force f versus undeformed contact line position y (Wilhelmy trace) for the rectangular defect. The shaded area represents the work of hysteresis. (c) Advancing and receding mechanisms.

Our samples were prepared by uv photopatterning [17] gold-coated cover slips (22 mm wide, 170 μm thick) with 11-mercaptoundecanoic acid (MUA) ("high-energy," $\theta_h = 35°$ or 15° for advancing or receding water) and 1*H*,1*H*,2*H*,2*H*-perfluorodecane thiol (FDT) ("low-energy," $\theta_l = 115°$ or 102° for advancing or receding water). Gold-coated substrates were immersed in 10^{-2} M MUA solution in ethanol for at least 1 h. The MUA self-assembled monolayer (SAM) was irradiated on a uv light table (254 nm) through a chromium mask on a quartz plate. The oxidized regions were then replaced with the FDT SAM by immersion in a 10^{-3} M FDT solution in ethanol for 2 h. Self-assembly of the FDT SAM was followed using x-ray photoelectron spectroscopy [17]. According to tapping mode AFM, the MUA-FDT boundary was <1 μm wide with no detectable physical step.

The Wilhelmy plate technique provides a suitable tool to generate a force-distance plot over an individual chemical defect. The plate position can be determined very accurately (μm), allowing the capillary force (down to 10^{-6} N) to be precisely mapped for a moving contact line, facilitating direct analysis of small pinning forces [18,19]. In this Letter, we present data for a series of defects varying in surface energy, size, and shape. All samples were immersed or emersed at 50 μm/s in a clean room (class 100). The influence of the immersion or emersion rate was studied to ensure that our results represented quasistatic conditions. Force data were collected at 0.1 s intervals, i.e., every 5 μm. One side of the sample was modified to include a single defect, while contributions from the rear of the sample were subtracted.

When a homogeneous plate is immersed into liquid, capillary rise or depression occurs depending on the wettability of the plate. The weight of the liquid meniscus is given by Eq. (2), where f is the capillary force, which is directly measured by the Wilhelmy balance [20] (after correction for buoyancy and the dry weight of the plate):

$$f = \gamma p \cos\theta. \tag{2}$$

If the perimeter of the plate p is sufficiently large, as in our measurements, the influence of the plate's edges is negligible. The basis for the Wilhelmy measurement is unchanged for a heterogeneous surface. Consider the rectangular defect in Fig. 1. The observed capillary rise h is the difference between the capillary rise on the high-energy defect and the capillary depression on the low-energy matrix. The measured force is simply the sum of the capillary forces acting on the plate:

$$f = \gamma[w \cos\theta_h + (p - w)\cos\theta_l], \tag{3}$$

where the effect of contact line curvature at the defect boundaries has been neglected [21]. In order to consider the defect alone, the background contribution from the matrix may be subtracted to give the change in force Δf upon liquid-defect contact:

$$\Delta f = \gamma w \Delta\cos\theta, \tag{4}$$

where $\Delta\cos\theta = \cos\theta_h - \cos\theta_l$. It should be noted here that Δf is independent of the height of the defect d provided $d > h$. From our experiments, we can confirm that Eq. (4) is generally applicable to the macroscopic defects studied in this Letter (see Fig. 2) whenever $d > h$. Alternatively, when $d < h$, the liquid is unable to reach its equilibrium capillary rise before arriving at the upper defect boundary, where it is pinned, reducing the measured value of Δf.

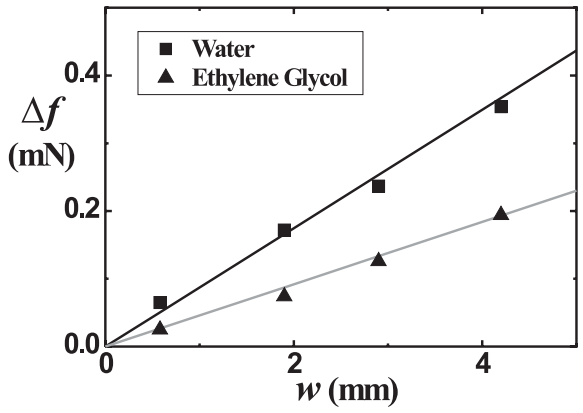

FIG. 2. Measured force difference Δf on rectangular high-energy defects as a function of the defect width w. The data agree with Eq. (4) for water, $\gamma = 72.8$ mN/m (black line), and ethylene glycol, $\gamma = 46.0$ mN/m (gray line).

A typical Wilhelmy trace for water advancing or receding over a rectangular high-energy defect is shown in Fig. 3, where $\Delta \cos\theta$ is approximately constant irrespective of whether or not the contact line is advancing or receding. We achieve this experimentally by appropriate preparation of the two surface components. Importantly, $\Delta \cos\theta$ differs between the advancing and receding measurements by less than 6%, almost negating the inherent hysteresis on each of the pure components. The measured trace generally follows that predicted by Joanny and de Gennes, Fig. 1(b) [14]. The spikes immediately following capture and detachment are due to the inertia of the liquid. The theoretical capillary rise is briefly exceeded until the overstretched interface relaxes back to the equilibrium position h. The observed capillary rise h and measured force difference Δf can be determined directly from the trace. The magnitude of Δf reflects the width of the defect according to Eq. (4); however, the capillary rise h is significantly reduced when the defect width is less than the capillary length [16].

Rather than focus on the magnitude of the hysteresis energy ΔW, we chose to study the advancing W_a and receding W_r work separately. This approach has been adopted elsewhere to evaluate the work of detachment for a sphere [19]. Figure 4 presents W_a and W_r for a series of rectangular high-energy defects ($w = 3.5$ mm, $d =$ 0.4–5.5 mm). As one intuitively expects, $W_a < W_r$ for every sample. Curiously though, the magnitude of W_r is in excellent agreement with theory based on the defect area, $|W| = \gamma A \Delta \cos\theta$. This implies that little additional energy is required to de-pin the receding liquid, and therefore, the origin of ΔW must principally lie in the advancing mechanism (for a high-energy defect). In order to confirm that this was a general effect, we measured W_a and W_r for high- and low-energy, rectangular and circular defects of dimensions ranging from 0.4 to 5.5 mm. Since the mechanism is reversed for low-energy defects, W_a is plotted for the low-energy defects together with W_r for the high-energy defects. All of these data collapse onto a single theory line, $|W| = \gamma A \Delta \cos\theta$, irrespective of the size, shape, or energy of the defects, Fig. 5.

Our results suggest a general principle for wetting hysteresis that is broadly applicable to the characterization and control of surface wettability. Specific departure from equilibrium theory, i.e., Cassie's equation, may be more strongly linked to high-energy defects in the advancing case and low-energy defects in the receding case. In practice, this behavior should present itself as asymmetric departure from Cassie's equation for a surface exhibiting defects of a single energy (with respect to the matrix); i.e., either the advancing or receding measurements will significantly deviate from theory, but not both. Such asymmetric behavior has been observed experimentally [6,7], but its origin has remained unclear. Therefore, we prepared chemically patterned surfaces of solely high- or low-energy defects at various area fractions for comparison with Cassie's law.

Square (20 μm) or circular (10 μm diameter) defects were arranged in a regular lattice using uv photolithography, as described earlier. Contact angles were measured with Millipore water (18 MΩ cm) using the sessile drop method. The reported angles represent an average of 5 or more measurements on at least three separate samples. These data are shown in Fig. 6 against Cassie's predictions, based on the advancing (gray line) or receding (black line) contact angles for each component [22]. As we found no apparent difference between the two defect geometries, we only distinguish between the two defect energies to simplify Fig. 6. For each defect energy (high or low), either the advancing or the receding data significantly depart from Cassie's theory, but not both. For high-energy defects, the advancing data (open squares) bend away from Cassie's

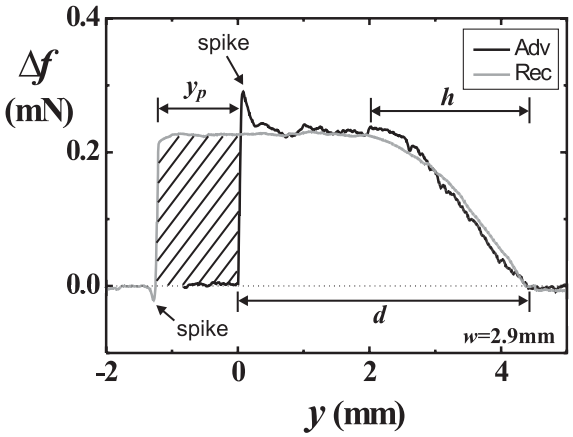

FIG. 3. Advancing and receding Wilhelmy traces for water on a rectangular high-energy defect ($d = 4.2$ mm, $w = 2.9$ mm). The shaded region represents the hysteresis work.

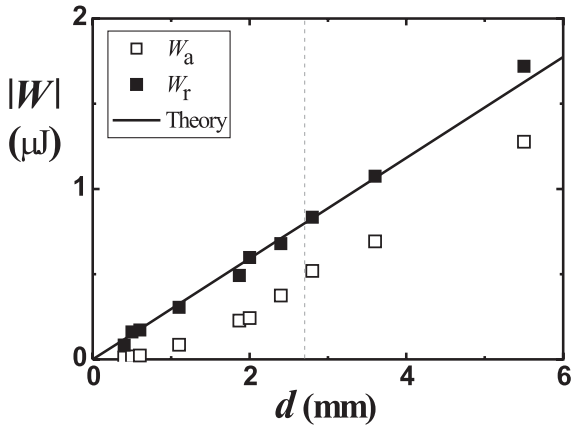

FIG. 4. Advancing W_a and receding W_r work for water as a function of the height of the high-energy defect d. The solid line represents the theoretical work based on the defect area, $|W| = \gamma A \Delta \cos\theta$. We observed close agreement between W_r and the theoretical work; however, W_a was shifted to lower values. The vertical broken line represents the defect height equal to the capillary rise, $h = 2.7$ mm for water. When $h > d$, W_r follows theory, while the slope of the advancing data is reduced.

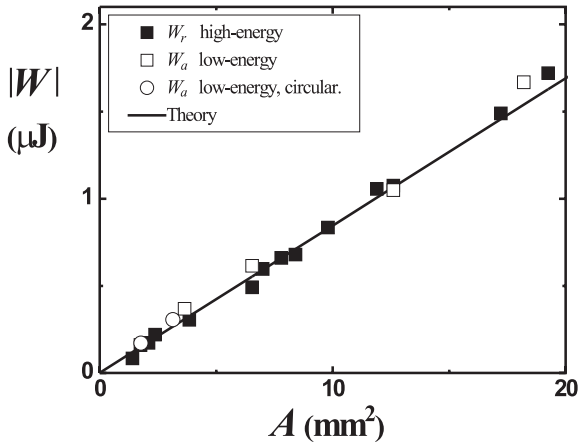

FIG. 5. Advancing work W_a for low-energy defects and receding work W_r for high-energy defects (for water) as a function of the defect area A. The solid line represents the theoretical work based on the defect area, $|W| = \gamma A \Delta \cos\theta$.

prediction to higher angles, whereas the receding data (open triangles) follow the theory closely. Conversely, for low-energy defects, the receding data (filled triangles) bend away from the theory to lower angles, while the advancing data (filled squares) follow Cassie's law. This ''asymmetric'' hysteresis, as we term it, is expected from our single defect measurements, but is seldom reported in the literature [6,7]. This is most likely due to the presence of both high- and low-energy defects (with respect to the matrix) on common heterogeneous surfaces, rather than of a single type as presented here and elsewhere [6,7].

In conclusion, we have investigated wetting hysteresis for individual rectangular defects. The measured advancing and receding work differed significantly, depending on the defect energy (relative to the matrix). For one, or an array of high-energy defects, our advancing measurements strongly departed from equilibrium theory, while the receding data were in quite close agreement. Conversely for low-energy defects, only receding measurements departed from theory. We propose that the distinct wetting behavior at high- and low-energy defects explains the phenomenon of asymmetric hysteresis, where the advancing or receding angle deviates more strongly from theory. We anticipate that this work will provide fundamental insight into the mechanisms controlling wetting of inherently heterogeneous surfaces and influence the design of synthetic interfaces for specialty wetting applications.

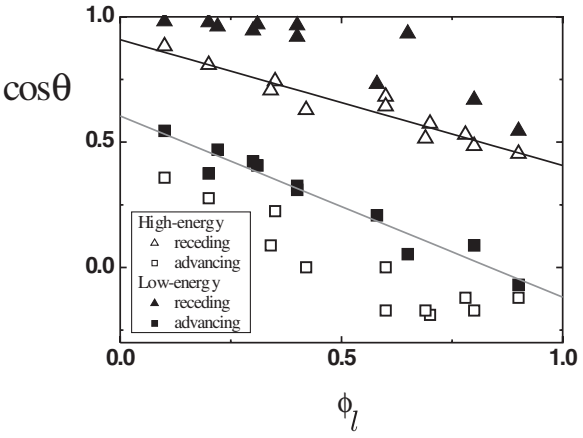

FIG. 6. Measured contact angles (water) against the area fraction of the low-energy component ϕ_l. When the data are fitted according to Cassie's law, Eq. (1), close agreement is observed for advancing data over low-energy defects (gray linear fit) and receding over high-energy defects (black linear fit). Conversely, significant departure from Eq. (1) is observed for high-energy defects when advancing, and low-energy defects when receding.

We thank Claudia Schäfle and Martin Brinkmann for insightful discussions. Financial support from the Australian Research Council Special Research Centre Scheme is acknowledged.

[1] L. Zhai *et al.*, Nano Lett. **6**, 1213 (2006).
[2] B. Zhao, J. S. Moore, and D. J. Beebe, Science **291**, 1023 (2001).
[3] T. Young, Phil. Trans. R. Soc. London **95**, 65 (1805).
[4] A. B. D. Cassie, Discuss. Faraday Soc. **3**, 11 (1948).
[5] R. Crawford, L. K. Koopal, and J. Ralston, Colloids Surf. A **27**, 57 (1987).
[6] V. de Jonghe and D. Chatain, Acta Metall. Mater. **43**, 1505 (1995).
[7] Y. V. Naidich, R. P. Voitovich, and V. V. Zabuga, J. Colloid Interface Sci. **174**, 104 (1995).
[8] S.-I. Imabayashi *et al.*, Langmuir **14**, 2348 (1998).
[9] J. T. Woodward, H. Gwin, and D. K. Schwartz, Langmuir **16**, 2957 (2000).
[10] T. Cubaud and M. Fermigier, J. Colloid Interface Sci. **269**, 171 (2004).
[11] D. C. Pease, J. Phys. Chem. **49**, 107 (1945).
[12] R. E. J. Johnson and R. H. Dettre, J. Phys. Chem. **68**, 1744 (1964).
[13] A. W. Neumann and R. J. Good, J. Colloid Interface Sci. **38**, 341 (1972).
[14] J. F. Joanny and P. G. de Gennes, J. Chem. Phys. **81**, 552 (1984).
[15] G. D. Nadkarni and S. Garoff, Europhys. Lett. **20**, 523 (1992).
[16] J. A. Marsh and A. M. Cazabat, Europhys. Lett. **23**, 45 (1993).
[17] M. J. Tarlov, D. R. F. Burgess, Jr., and G. Gillen, J. Am. Chem. Soc. **115**, 5305 (1993).
[18] M. E. R. Shanahan, Surf. Interface Anal. **17**, 489 (1991).
[19] O. Pitois and X. Chateau, Langmuir **18**, 9751 (2002).
[20] L. Wilhelmy, Ann. Phys. (Berlin) **195**, 177 (1863).
[21] T. Pompe and S. Herminghaus, Phys. Rev. Lett. **85**, 1930 (2000).
[22] The contact angles for the pure components in Fig. 6 differ from those stated earlier due to slight changes in our lithography method, but do not adversely affect the basis of our conclusions.